

## Article

# Water Balance Trends along Climatic Variations in the Mediterranean Basin over the Past Decades

Zaib Unnisa <sup>1,2,3,\*</sup> , Ajit Govind <sup>2</sup>, Bruno Lasserre <sup>3</sup>  and Marco Marchetti <sup>3</sup> 

<sup>1</sup> Department for Innovation in Biological, Agri-Food and Forest Systems (DIBAF), University of Tuscia, 01100 Viterbo, Italy

<sup>2</sup> International Center for Agricultural Research in Dry Areas (ICARDA), Cairo 11435, Egypt

<sup>3</sup> Department of Biosciences and Territory, University of Molise, 86090 Pesche, Italy

\* Correspondence: zaib.unnisa@unimol.it

**Abstract:** The heterogeneous ecosystems in the Mediterranean Basin (MB) are becoming sensitive to water stress. To investigate the climatic stress, a water budget study was conducted over the basin using TerraClimate simulations for a long temporal range (1990–2020). According to the budget accounting, forested regions received the highest precipitation (P) on average compared to other land use types (annual mean  $\approx 633$  mm yr<sup>-1</sup>), and even then, they were in a water deficit state ( $-0.42$  mm yr<sup>-1</sup>). Tree plantations in North Africa (Libya and Morocco) were also in a water deficit state; however, their average P was very low ( $\approx 12$  mm yr<sup>-1</sup>) compared to that of northern parts of the MB, and the average Actual Evapotranspiration (AET) was  $\approx 15$  mm yr<sup>-1</sup>. Also, the water balance in other land use systems (rain-fed, irrigated croplands, and rangelands) was either negative or near zero. As a whole, the basin's average annual P was  $\approx 538$  mm yr<sup>-1</sup>, the annual average AET was  $\approx 415$  mm yr<sup>-1</sup>, and the runoff (Q) was equivalent to 123 mm yr<sup>-1</sup>, which shows a strong influence of ET over the region. Since runoff was negligible in most dry areas, the AET's large contribution was notable in the North African base of the Atlas Mountains including the Nile delta region. This indicates that precipitation and evaporation are the principal mechanisms of the water balance in the MB. The result shows strong climate variability over Southern Europe, Turkey, and the western Balkans in the recent years, affecting the AET and making their land use systems more vulnerable to water stress. This benchmark study signifies the consistent need for water storage in the Mediterranean vegetation systems of the basin. It also indicates two distinct climate clusters for water balance modeling.

**Keywords:** Mediterranean basin; climate fluctuations; water deficit; Mediterranean ecosystems; Budyko curve



**Citation:** Unnisa, Z.; Govind, A.; Lasserre, B.; Marchetti, M. Water Balance Trends along Climatic Variations in the Mediterranean Basin over the Past Decades. *Water* **2023**, *15*, 1889. <https://doi.org/10.3390/w15101889>

Academic Editors: Alban Kuriqi and Luis Garrote

Received: 9 January 2023

Revised: 7 March 2023

Accepted: 12 March 2023

Published: 16 May 2023



**Copyright:** © 2023 by the authors. Licensee MDPI, Basel, Switzerland. This article is an open access article distributed under the terms and conditions of the Creative Commons Attribution (CC BY) license (<https://creativecommons.org/licenses/by/4.0/>).

## 1. Introduction

In the Mediterranean climate, changes to freshwater availability directly affect total annual precipitation volumes. A rise in temperature also increases the evaporative demand. These effects bring variations in the water balance of the MB, and their frequent monitoring is significantly important to maintain socio-economic balance in water use and distribution. Such long-term monitoring also helps in understanding the nature of hydro-climatic fluctuations in the basin, which can also be human evolved. However, climatic effects are the prime contributor to the hydrological imbalances in the arid and semi-arid production systems of the MB, as these systems are more vulnerable to freshwater decline. Recent studies envisaged that the MB would experience an aridity of more than twice its present extent with future climate changes [1,2]. An increase in drought frequency and warm spells has also been documented in the MB in the last 40 years (1979–2018) [3,4]. These dry weather events are predicted to be more pronounced in hyper-arid regions like North Africa, southern Spain, and the Middle East [5]. Frequent dry spells, especially during the

crop growing season, can increase water demand and can make basin ecosystems more sensitive to water stress [6]. Changes such as late springs, coupled with freshwater decline, are already affecting the net ecosystem productivity of the basin [7]. By 2050, the MB will experience more water deficit with a 30–50% decline in freshwater resources [8]. In such a case, an accurate assessment of the water budget is extremely important to conduct and control supply and demand imbalances.

Many studies found Evapotranspiration (ET) as an important hydrological flux in context with surface and deep surface responses to climatic variations [9,10]. It is also a principal water-extracting component in the most arid regions, and its accurate quantification along with precipitation is becoming more critical with the growing water scarcity in the basin. Several studies assessed the Mediterranean water budget using ET at various scales with a variety of projections and methodologies, i.e., Med-CORDEX [11], the Weather Research and Forecasting model [12], the bucket with a bottom hole (BBH) model with RCMs SMH-E and SMH-B [13], the LPJ model [14], and the transient model [15]. A few studies used the water budget equations with additional parameters, or the runoff or ET estimation at basin scale, while some modified water balance methods for region-specific studies in order to carry out the water budget explicitly [16–21]. Usually, in the majority of water budget estimations, the interpolated or gridded datasets of precipitation (P), actual ET (AET), and runoff (Q) are used, which are either simulated with climate or hydrological models or derived from reanalysis climate data. Some studies compared the budget inferences from different data sources and compared their associated uncertainties or absolute errors in budget estimates. Since the accuracy in estimations is a priority in hydrological assessments in order to set reliable benchmarks for long-term water management, it is necessary to account for and fix large errors in budget closures with associated uncertainties. For this study, we used the recently released monthly TerraClimate product for the water budget evaluation and Budyko curve analysis to investigate the water-limited state in different parts of the basin. We also assessed the water stress conditions in various land uses (wetland, agriculture, forest, and urban) at a plausible resolution (1 km). The TerraClimate product has already gained confidence in various hydrological assessment studies, i.e., in closing a water budget [18], freshwater flux differences [22], the impact of extreme events on the budget [23] and has also been validated with in situ data in various locations.

The terrestrial water budget is mainly constrained by energy and water limitations. These limitations are determined by the simple Budyko hypothesis. This technique is robust for evaluating water resources [24] in data scarce regions at various scales, i.e., global [25,26], national or large river [27], and basin-scale [28,29]. It relates the long-term average of a basin's actual evapotranspiration (AET) to its potential evapotranspiration (PET) and precipitation (P) in a semi-empirical way. It has many applications in hydrological studies; for instance, Li and Quiring (2021) [30] used the Budyko framework to investigate spatial heterogeneity in the factors that control the water balance, while looking at the importance of forest coverage as a function of climate. Wang and Hejazi (2011) [31] developed a decomposition method using the Budyko framework, to link discharge variability with hydrological components. Xu (2011) [32] also used a Budyko-like framework to develop a regression model and decompose the contribution of anthropogenic activities to the reduction of water resources in a basin. Our study quantifies the current nature of the water balance at the annual time step, using a first-order water balance approach and a Budyko framework to derive clusters with terrestrial water balance components. We also accounted for potential water storage differences among the existing land use patterns in the MB. The results may be used as a benchmark for tracking the changes in the water budget after the 1991–2020 period, and may assist decision-makers in setting future targets for water storage in the basin.

## 2. Materials and Methods

This study used monthly TerraClimate datasets for computing the 30-year average water budget using three principal hydrological components: P, AET, and Q. TerraCli-

mate is mainly derived from Climate Research Unit CRU 4.0 [33], in substitution with Japanese reanalysis JRA55 data, which are particularly used for sparse station regions such as Africa. The hydrological flux components (AET and Q) were calculated via a modified Thornthwaite-Mather climatic water balance model, wherein storage or drainage is constrained with the defined soil water storage capacity with the lookup table method. The Thornthwaite-Mather climatic water balance model uses the relation of P, PET (calculated using the Penman-Monteith equation), soil moisture, and snowpack water storage to compute the water balance. In this case, some of P is intercepted by the canopy and lost through evaporation. The remainder, i.e., throughfall, is added to the soil water pool. When the resulting volumetric soil water content exceeds the capacity of the soil, this excess is deemed to be lost as runoff or drainage (Q), which is used in this analysis.

All of these components were validated from station data and streamflow gauges [34]. The product has better spatial realism (4 km) and quality in terms of average absolute error than its older versions. The details on the TerraClimate product development are in [35].

The entire 30-year budget calculation (1991–2020) was conducted in the google earth engine (GEE) platform (source code and datasets are available). Potential and actual evapotranspiration, runoff, and precipitation products were rescaled with 0.1, and all were resampled to 1 km resolution using the bilinear resampling method embedded in GEE. To quantify the water surplus and deficit state of basin's land use systems, the most recent Mediterranean Land System Map (2017) was used. The details of the dataset are given in the Table 1 below and the land cover classification methodology is discussed in [36].

**Table 1.** Datasets used for trend analysis and the water budget calculation for the study period (1991–2020).

Dataset	Variable	Spatial Resolution	Source
Terraclimate, University of Idaho	Precipitation Potential Evapotranspiration (ASCE Penman-Montieth) Actual	4.6 km resampled 1 km	Abatzoglou et al. 2018 [35]
Mediterranean land systems	Evapotranspiration Runoff 26 land cover types	2 km resampled 1 km	Malek and Verburg, 2017 [36]

The PER method used in this study provides temporal variability of water budget changes using P, E, and Q [21]. In this method, the continuity equation gives the change in the storage within a specific area by subtracting the input precipitation from output sources (evapotranspiration and runoff), over the territory only.

$$P - Q - E = \Delta S \quad (1)$$

where P = precipitation, Q = runoff, E = evapotranspiration, and  $\Delta S$  = water storage.

The annual averages were computed for these three water balance components within the basin domain. Then, the class-wise average value of each component was retrieved to find out which regions and land use land cover systems were in a water deficit state. To understand regional water trends, the basin was subdivided into four regions to compare annual budget time series; the sub-division is shown in Figure 1. Later, a simple Mann-Kendall statistical test was applied on annual datasets to assess whether the budget and its components were increasing over time or decreasing, and whether the trend in either direction was statistically significant. In last, the Budyko framework [37] was applied at the mean annual time scale to find aridity clusters in the basin.

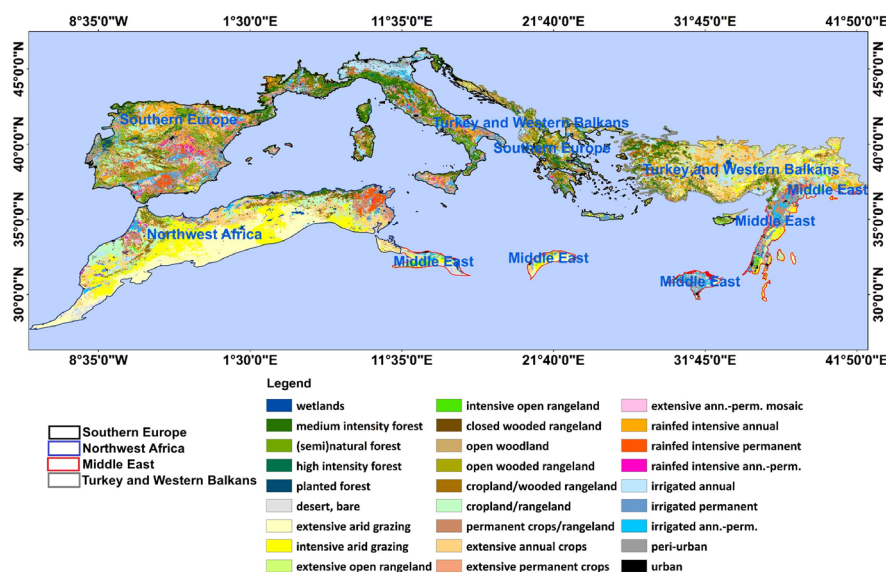


**Figure 1.** Diverse land systems in Mediterranean region with 26 thematic classes representing intensive and extensive typologies of forests, crops, wetland, agro-pastoral, and grazing systems lying in the four sub-regions differentiated with colored outlines, i.e., Southern Europe (black), Northwest Africa (blue), Middle East (red), and Turkey and Western Balkans (grey).

### 2.1. Budyko Curve Theory

The Budyko technique sets a semi-empirical relation between the evaporative index,  $AET/P$ , and the aridity index,  $PET/P$ . This relation can be termed as the Budyko  $AET/P$  versus  $PET/P$  curve, and is a conventional metric of climate aridity, often used to identify regions under climatic water deficits. In this technique, the annual water balance can be expressed as a function of the available water and energy, and the ratio of the mean annual evaporation to the mean annual precipitation ( $E_a/P$ , evaporative index) is manifested by the ratio of the mean annual potential evaporation to the mean annual precipitation ( $E_0/P$ , dryness index). If the dryness index is less than one, it means that the energy supply is the limiting factor for evaporation; if it is greater, then the water supply is the limiting factor. These indexes are typically affected by climate seasonality, topography, soil types, and vegetation. Yu et al. 2021 [38] revealed that vegetation coverage had a dominant effect on  $AET$  changes, while climate seasonality that has a negative effect on  $AET$  had a relatively lower effect. This indicates that vegetation dynamics can change the water budget situation in the basin, but at this broad region scale, our focus was to investigate the storage and consumption of water in the current land use system considering the atmospheric supply only. Landscape dynamics can only be assessed with the availability of a dynamic land use land cover (LULC) with a similar typology, which is missing in this study. Since the region is so diverse, 90% accuracy in LULC assessment is difficult to achieve.

### 2.2. Land Use Systems in the MB

In this study, the recent land use land cover map used represents the vegetation of 27 countries, covering an area of 2.3 million  $\text{km}^2$ . The basin surrounding the Mediterranean Sea has similar climatic and biophysical traits. In previous studies, the Nile River basin was usually not considered as being part of the MB, with the reason being that the source of this transboundary basin is in the tropics, and its tropical hydrological regime and water management issues go beyond the Mediterranean context [8]. Now in the new classification map, the Nile Delta and Apennines forests of Italy are included, with the justification of their sharing of common Mediterranean ecoregions falling in the Middle East and Southern European regions.

These 26 land cover classes shown in the map (Figure 1) were derived from land cover, livestock density, irrigation extent, and different intensity proxies' information from

existing databases, using expert-based hierarchal classifications; the detailed methodology is given in [36]. This map is specifically used because of its significantly improved thematic typology at a higher resolution (2 km) compared to existing land cover products.

It sufficiently represents variations in the land systems across the region and gives a realistic view of climatic impacts on landscapes, compared to other classified maps. As the distribution indicates, a majority of intensive rain-fed systems exist in Spain, intensive and extensive arid grazing systems in North Africa, and a majority of irrigated croplands exist in Italy and Egypt. Forests are more common in Italy and Scandinavian countries, while Turkey, Spain, and the Balkans have a majority of rain-fed cropping systems and fewer forests. Their areal densities are given in Table 2, and the sub-regions shown in colored borders are used for further investigation on the water budget.

**Table 2.** Annual average of hydrological components for land use land cover classes.

Major Class	Area %	P (mm yr <sup>-1</sup> )	AET (mm yr <sup>-1</sup> )	Q (mm yr <sup>-1</sup> )	ΔS (mm yr <sup>-1</sup> )
Bare and Open Grazing systems	22.6%	486.96 ± 110	359.32 ± 58	127.61 ± 69	0.18 ± 28
Cropland Systems	37.9%	540.56 ± 111	429.60 ± 63	110.91 ± 65	0.00 ± 36
Forest systems	10.1%	633.63 ± 125	463.56 ± 62	170.88 ± 80	−0.42 ± 36
Agro-silvo pastoral mosaics	23.3%	633.41 ± 133	479.99 ± 68	153.62 ± 86	−0.41 ± 41

### 3. Results

This study examined the water balance of diverse land use systems in the MB, in which a 30-year average trend was determined for the Mediterranean ecosystems in the spatial domain of four major regions surrounding the Mediterranean Sea: Europe, North Africa, the Middle East, and Turkey and the Balkans (Figure 1). The geographical location, climatic zone of the sub-region, and various spatial and temporal processes can all affect the overall water balance of the basin. In areas where rainfall is scarce, the major inflows come from the sea (desalinated water) into the terrestrial ecosystem. However, only P could be accounted here as main inflow. On the other hand, evaporation from water bodies is also considered negligible, which is often true in arid and semi-arid areas at the coarser resolution; thereby, AET from vegetation was taken as the main outflow component. In this study, we analyzed the basin's average budget state in the current climate conditions, while exploring the significance of ET in the arid and semi-arid land systems through trend analysis. Such analysis is essential to understand a basin's behavior, priorities, and needs.

As can be seen in Figure 2, the average P was spatially distributed between 2413 and 12 mm yr<sup>-1</sup>, with the lowest in Egypt and entire North African belt (less than 200 mm yr<sup>-1</sup>). The latter is comparable to the 1979–1999 period-averaged precipitation map found in [39]. While the maximum amount of rain was confined to small areas in Italy, the Balkans, and coastal areas of North Africa and Spain, as expected, the basin showed contrasting humid and arid climate compositions. In the northern regions, the P was >1000 mm yr<sup>-1</sup> and PET < 1000 mm yr<sup>-1</sup>; in contrast, the southern regions had a P of <300 mm yr<sup>-1</sup> and a PET of >1000 mm yr<sup>-1</sup>. The surplus water was available mostly in the coastal regions of Lebanon and Israel, and parts of the Middle East, while the majority of the basin had a storage of nearly −0.5–2 mm yr<sup>-1</sup>, which indicates a critical water deficit at an annual time step in a large part of the region.

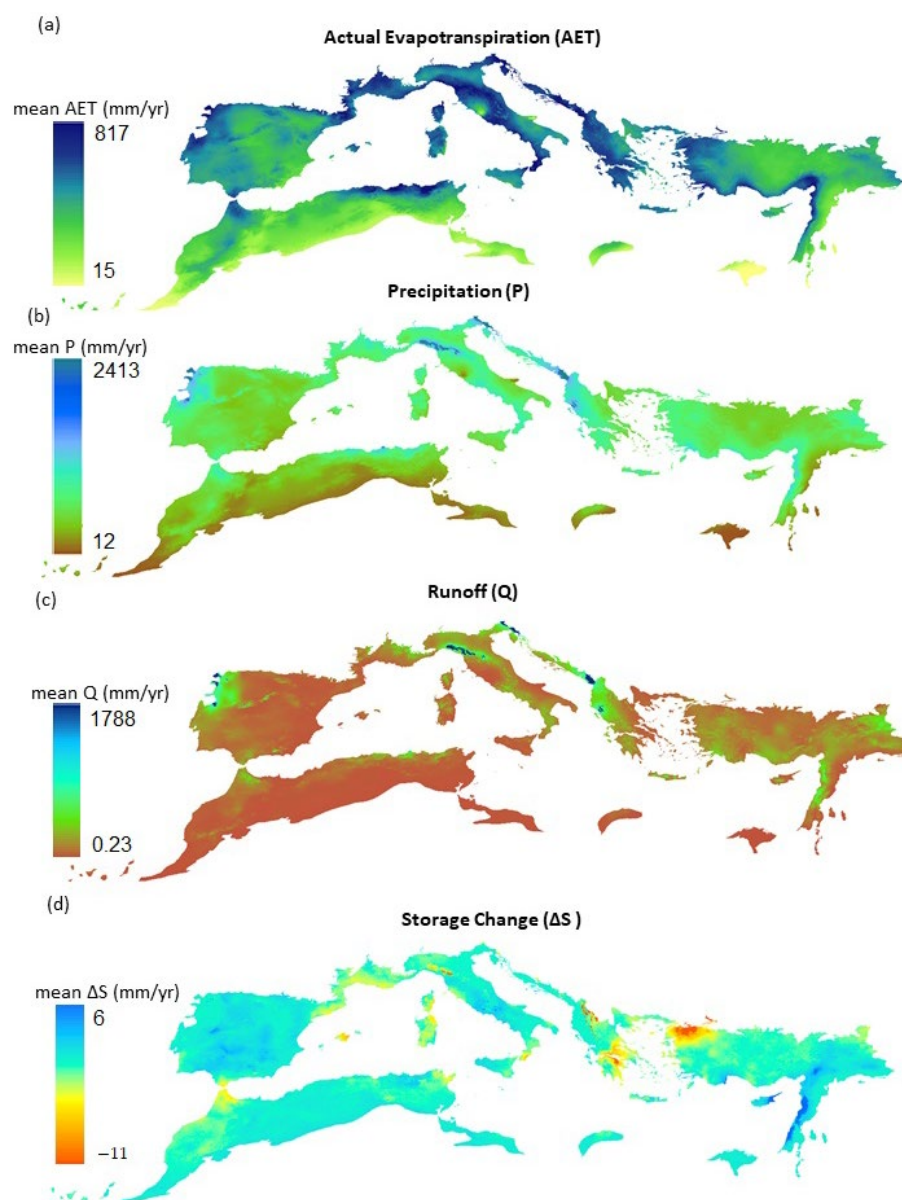


**Figure 2.** Shows the spatially averaged map of (a) actual evapotranspiration (AET), (b) precipitation (P), (c) runoff (Q) (d) water budget for the 30-year period (1991–2020).

In comparison with the AET annual averaged map, a similar pattern was found, in which areas where P was above  $1000 \text{ mm yr}^{-1}$  also had an AET greater than  $500 \text{ mm yr}^{-1}$ . The gap between P and AET was very close for North Africa, especially in Egypt.

After applying the first-order water budget Equation (1), an extreme water deficit of nearly  $-11 \text{ mm yr}^{-1}$  was found in Greece, Albania, and the northwestern part of Turkey where the Kōroğlu mountains exist. This large water deficit over Greece and Turkey could have been a stimulus for the extreme wildfires that were spotlighted in the international media [40,41]. Wildfires could be a consequence of increasingly drier conditions over the Mediterranean region. We also identified the Balkans, Maghreb, North Adriatic, Central Spain, and Turkey as the most affected regions from frequent wildfire events, and consider them to be under a climate crisis. Reduction in the stream flows are noticeably impacted by climate change, this observed deeply at the catchment scale in Catalonia, Spain [42]. Another scientific reason for the water deficit could be orographic effects in the mountainous region, where increased evapotranspiration rates at the peaks makes more water available for vegetation at foothills, and simultaneously less water available for transpiration in the

mountains, making the water deficit more prominent over the peaks. As the annual average of ET and Q cannot justify the reasoning fully, neither lateral distributions are accounted for in this analysis. To justify this deficit, available water in the form of infiltration and groundwater is also required in the budget analysis, as Freund and Kirchner (2017) [43] considered  $P + \text{net lateral transfer}$  to quantify its effect on average ET; they found that ET increases when the dryness index increases with altitude, due to the lateral movement of water from more humid uplands to more arid lowlands. It shows that lateral water transfers will strongly affect the average ET if the source (or recipient) location is energy limited and the recipient (or source) location is water limited, which is not accountable with the existing Thornthwaite water balance approach. Overall, the runoff (Q) and P have similar spatial patterns, which indicates areas where P is more allocated to the mountainous systems which have greater runoff, and also highlights the near-zero runoff condition in the majority of the downstream basin areas. This situation will increase in the future, and the zero runoff condition will markedly increase with a decreasing P influx, as a notable decrease in streamflow is also suspected for the period 2076–2100 in the Mediterranean region, as predicted via climate modelling [40].

This spatial pattern (Figure 2) was further analyzed with a recent and detailed high-resolution land use land cover map, and it indicated that all types of vegetation on average were under a water-deficit state (Table 2). Surprisingly, forest and pastoral systems spreading over the entire basin showed on average a negative water balance. Medium intensity forests, followed by bare areas, received the highest precipitation on annual average among all land cover types. The class-wise statistics also showed the prominence of ET in the water budget of the basin. Cropland systems that had the highest distribution of nearly 38% in the basin had an average water budget close to zero, and were especially negative in the irrigated systems. Even forests covering just 10% of the land had a negative water balance. This clearly shows that Mediterranean vegetation systems are under climate-induced water stress. In fact, in all land use systems, the water storage situation was either negative or zero in average conditions, which can be seen in the minor classes as well (Appendix A). This was further observed in the graph of LULC systems that showed the minimal difference between inflow and outflow (Figure 3).

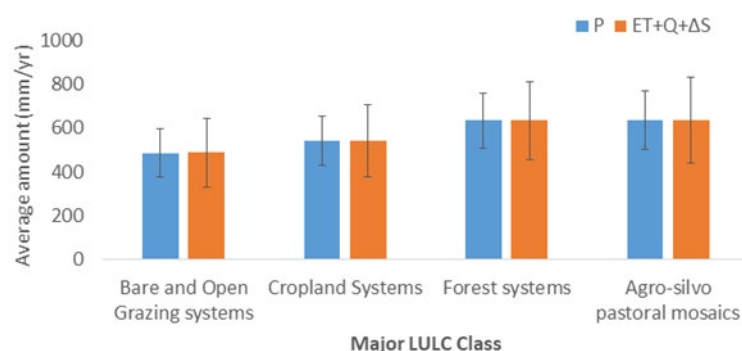


**Figure 3.** Inflow and outflow budget differences close to zero, among major land use land cover class of the MB.

This water-limited state was further verified with the Budyko framework that represents a simple first-order relationship among hydrological components. In this regard, each region's annual averaged evaporative and dryness index was plotted over the Budyko curve. Some interesting clusters formed with the sub-regional study that clearly justifies regional climatic differences in the Budyko curve. The majority index values found in the water-limited region of the Budyko curve in the horizontal direction indicate the dominant climatic influence on the hydrological cycle in the basin, as the basin is getting warmer and drier over time. Southern Europe (SE), Turkey, and the west Balkans showed more similarity in their chronological patterns for PET while showing a diagonal position on the curve; these regions are indicating a relatively less constrained state by available water

supply, compared to the Middle East and Northwest Africa, where climate variability is more pronounced with a dispersed pattern and is highly constrained by water limitations.

North Africa's closeness to its water limit is shown in Figure 4, which depicts its fragility and vulnerability to a dry climate far greater than other regions. Nevertheless, this analysis covers only the Mediterranean region under thick or sparse vegetation. The climatic effects on vegetative parts are obvious from declining productivity and growing food insecurities in the region.

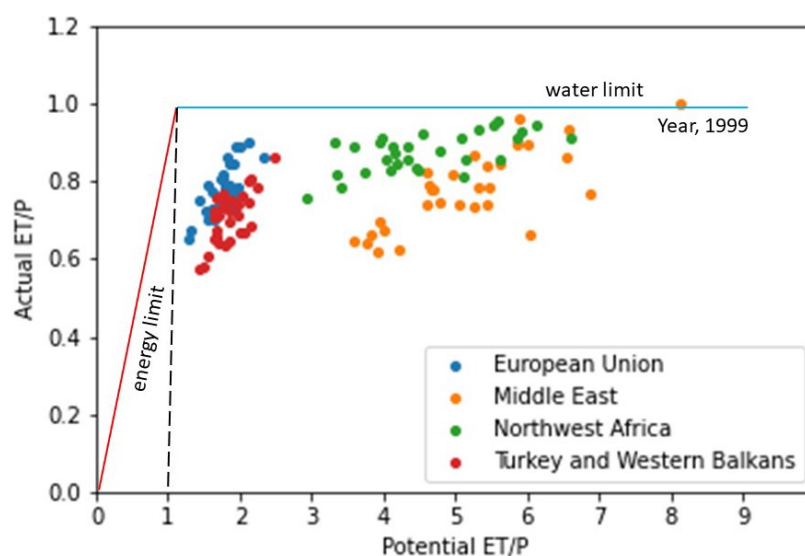


**Figure 4.** The dots represent the distribution of the mean annual evaporative index (E/P) versus the mean annual dryness index (PET/P), accounting for the TerraClimate averages over the 30-year period for the MB. The red and blue lines are the hypothetical water and energy limits of the Budyko framework.

The time series of hydrological components for the thirty years (1990–2020) were computed to observe the climate variability in each region. The region-wise stacked time series of P, AET, Q, and  $\Delta S$  revealed that synchronicity exists between temporal averages of AET and P because this basin area is mostly covered with vegetation. However, the P and AET ranges vary with the regions, as the Middle East and northwest Africa have both a lower P and AET in the comparable range of 200–400 mm yr<sup>-1</sup>. The gap between the average P and AET trend lines is lesser than the difference gap found in SE and the Turkey and the Balkans regions, where runoff is more prominent and generally highest (Figure 5). Davraz et al. (2014) [44] also found rainfall to be a prominent cause for the surface water level increase in Turkey, with direct and indirect recharges through runoff. It also indicates that the runoff varies by region in the basin, which is also linked to the AET distribution. The average precipitation peaks for SE and NA are chronologically similar (1996, 2003, 2010, 2018), indicating that extreme precipitation events happen after every seven or eight years. The years 2003 and 2018 are also important in terms of the peak found in the Middle East, the Balkans, and Turkey. The difference gap between AET and P in SE and Turkey and the Balkans is larger because of the prominent runoff trend ranges between 0 and 300 mm yr<sup>-1</sup>, their AET average ranges between 400 and 500 mm yr<sup>-1</sup>, and P between 600 and 800 mm yr<sup>-1</sup>. This trend analysis indicates the regional differences in the water budget components, with more water storage fluctuations in the Balkans and Turkey followed by Southern Europe. The water budget in these regions is also close to zero and negative in some places, which means that much of the precipitation consumed in the basin and annual variability in storage is greater than that of the MENA region. By noticing temporal signals, more climate fluctuations in terms of precipitation can be observed in the recent decades, especially for Southern Europe, Turkey, and the Balkans. Ajjur and Baalousha (2021) [45] also observed substantial changes in the components of

the hydrological cycle, which has increased the imbalance between the water supply and demand across the MENA region. According to climate projections for the middle and end of century (2021–2050, 2071–2100), temperature rise is the principal reason for PET losses that amplified the AET, which in result reduced the water availability in the MENA region [10] (Ajjur and Al Ghamdi 2021). In Europe, Deszi et al. (2018) [46] identified AET as an important driver of water availability, and their future projections over Europe postulated a pronounced water deficit in Southern Europe with reference to an ET increase. This also supports budget inferences, and testifies growing hydrological constraints in the current climatic conditions.

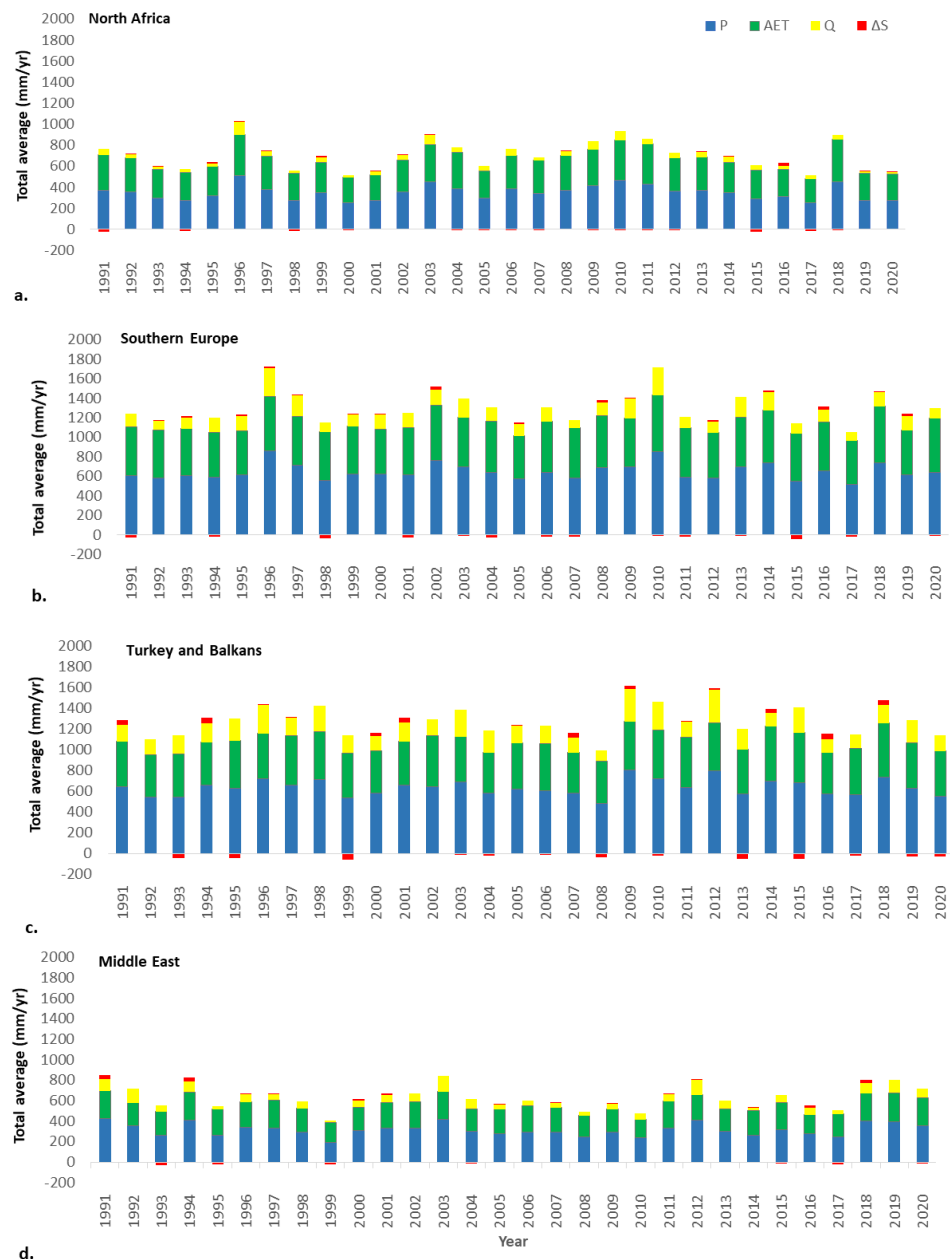


**Figure 5.** Annual average moisture budget over four regions for 1990 – 2020. Given are annual averaged trend of precipitation (blue), evapotranspiration (green), runoff (yellow) and minus change in terrestrial water storage (red), for (a) North Africa (b) Southern Europe (c) Turkey and the Balkans (d) Middle East.

Figure 6 shows a clear demarcation of latitudinal similarity among the four sub-regions in the temporal trends of the budget components. SE and Turkey and the Balkans have

shown similar magnitudes in P and AET with some variations in peak years. Trendlines of all budget components showed a similar trend of a slight uplift in AET and P, while also a statistically insignificant decreasing trend found in SE, via the Mann Kendall test (Table 3). No trend was observed in most cases, which indicates only a very slight change in the behavior of the basin.

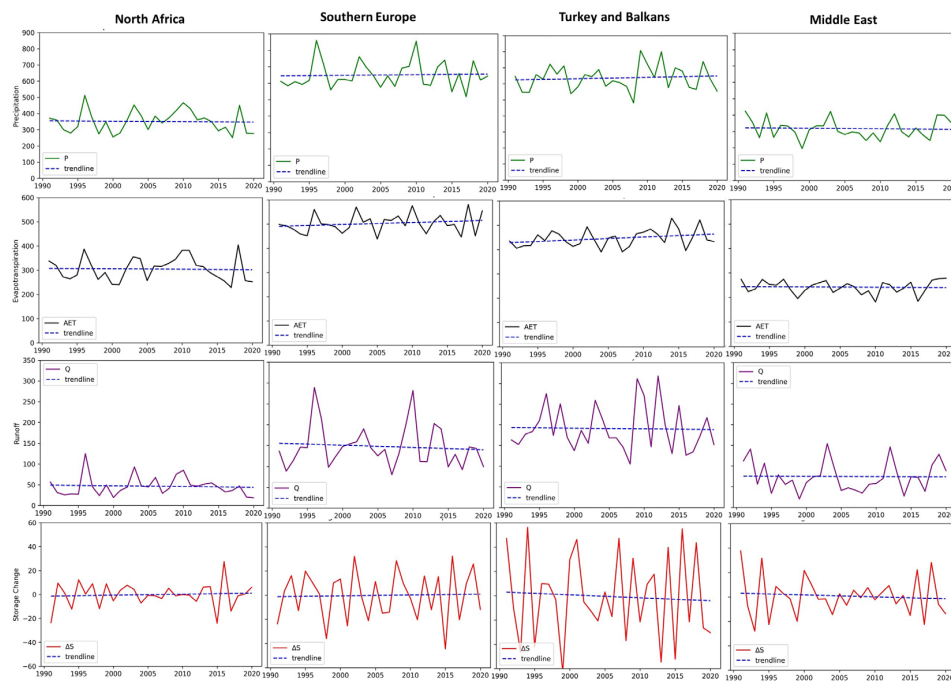


**Figure 6.** Long-term time series of water budget components over four sub-regions, i.e., North Africa, Southern Europe, Turkey and the Balkans, and the Middle East, with their averaged trend behavior.

The entire region observed a peak in the P and a storage change in the recent year 2018, which was also noticed as a year of climate extremes (drought and heavy precipitation) in North Africa [47]. Overall, the time series graph shows greater hydro-climatic fluctuations over SE, Turkey and the Balkans, indicating that climate predictions could be more uncertain and challenging here. As AET accounting is based on the water balance approach, wherein a significant part of irrigation and external water sources is missing and is not visible in the Middle Eastern Nile region as well, it could affect budget studies with conventional techniques. Remote sensing-based ET computations should be included in the budget assessments in future budgeting to account for irrigated ET. However, this study is primarily based on the terrestrial water budget, in which P is the main inflow and AET is computed following a one-dimensional simplified water balance approach explained in the methodology section. This first-order water balance calculation could reveal the storage condition on an annual basis in the major land use systems in the region, which are elaborated in this study in different ways.

**Table 3.** Mann-Kendall test results.

Sub-Region	P				AET				Q				ΔS			
	Trend	S Statistic	Z	p-Value	Trend	S Statistic	Z	p-Value	Trend	S Statistic	Z	p-Value	Trend	S Statistic	Z	p-Value
North Africa	no trend	−6	−1.22	0.22	no trend	−6	−1.22	0.22	no trend	−6	−1.22	0.22	no trend	4	0.73	0.46
Southern Europe	no trend	2	0.24	0.8	decreasing	−10	−2.2	0.02	no trend	4	0.73	0.46	no trend	6	1.22	0.22
Turkey & Balkans	no trend	0	0	1	no trend	4	0.73	0.46	no trend	8	1.714	0.086	no trend	−2	−0.24	0.8
Middle East	no trend	−4	−0.73	0.46	no trend	0	0	1	no trend	−6	−1.22	0.22	no trend	−4	−0.73	0.46

#### 4. Discussion

Like in other studies, we also found the highest precipitation (more than 1200 mm) to be over the Adriatic coast, the Alpine region, and over the coast of Turkey and the Atlantic Iberian Peninsula. The lowest precipitation was found in the southeast region of the basin, over the southern Iberian Peninsula, and over the northern coast of Africa, with less than 400 mm of precipitation. Past studies determined that precipitation changes in the MB are partially influenced by North Atlantic Oscillations (NAO), upon which their vegetation dynamics and compositions are based. Precipitation is significantly correlated with the NAO, which is known to be the primarily responsible atmospheric event for budget fluctuations; however, no significant correlation has been found for evaporation yet [48]. Besides that, there could be multiple factors that act together and contribute to the basin's hydrological responses. They could be region-specific characteristics, topography, geography, location, or precipitation regimes; however, their proportional influence has not yet been accounted for in the basin. A recent study indicated that the incoming P flux mostly comes from sources inside the Mediterranean. This proportion is only 35%, while 10% is from ET over nearby land in continental Europe, and 25% originates in the North Atlantic. The remaining 30% comes from the tropical Pacific or the Southern Hemisphere, indicating its direct connections with multiple locations on earth due to a global terrestrial energy redistribution. Therefore, fluxes have a more global than regional influence that links climate change effects with the water cycle in the basin [49,50].

As also noticed over Turkey and the west Balkans (Figures 5c and 6), hydro-climatic fluctuations are projected to increase, which would decrease annual precipitation in the southern Europe–Turkey region and the Levant, while in the Arabian Gulf area precipitation may increase. Besides that, daytime maximum temperatures appear to increase most rapidly in the northern part of the region, i.e., the Balkan Peninsula and Turkey, which means more evaporation. This will have marked effects on the ecosystems' productivity and functioning, as seen in the analysis. Moutahir [51] also noticed negative trends in the different water balance components, although they focused on the pine stands in the sub-humid belt of Spain; according to their budget analysis, the native pine population is likely to disappear in the future under extreme climate scenarios of water stress. The water-limiting conditions in the region are threatening for native tree plantations. Even the small quantity of water used by trees is important in the hydrologic budget of the Mediterranean areas where rainfall is limited; this indicates how significant the accurate computation of AET is in the budget [52]. In these regions, AET is mostly found to be higher: more than 54% of total precipitation, and mostly where tree density was lower [53]. This also shows how crucial precipitation is for forest growth and how it can control regional forest expansions or declines. Since many projected studies revealed that rainfall frequency is likely to be lower in the future, it would reduce the chances for aquifer recharge, despite their increasing size with extreme rainfall events. Changes in the precipitation intensity, size, and temporal distribution are expected in this region, and will have different effects on the water balance. Even in older studies, after precipitation, evaporation is recorded as the largest term in the Mediterranean freshwater budget in the 50 years of one study period (1948–1998) [48]. They also found that the Mediterranean region was under a freshwater deficit at the annual scale. The decrease in open water evaporation under future climate scenarios as a result of increased relative humidity will have a positive effect on the water cycle, but this trend would be seasonal and common in the winter only.

The goal of this paper was to provide a picture of the mean annual water budget along with the long-term variability of hydrological fluxes in the MB. It also justifies that complex morphology and climate variability contribute to significant annual differences in total precipitation and its geographical distribution. Rainfall and surface inflows (streams and rivers) are the major inflows, whereas evapotranspiration from different land uses and drains from the region to sea are the major outflows. A recent in situ study in Italy also validated our conclusion about the deficit state of the basin. They found a negative trend in the estimated infiltration for the consecutive five hydrological years (2017–2022). This

infiltration decrease was associated with a decrease in precipitation; however, they found AET in a less significant negative trend in the same period. This affirms that climate stresses are dominant in the MB, and that reduced surface water input will affect the groundwater input as well [54,55]. Scarascia-Mugnozza et al. [56] measured the hydrological balance at different integration times and found evapotranspiration was correlated to the water status of soils and plants. The indicated water stress can affect carbon metabolism, the water relations of forest trees, and ecosystem stability. All in all, AET was found to be an effective measure. This study highlights that both the accounting of the water budget at multi-scale and multi-functional systems are very important in considering the significant climatic influence over the water cycle and the budget. These findings could facilitate future climate preparedness and monitoring tasks.

## 5. Conclusions

This study attempted to investigate long-term water budget trends in the basin using only TerraClimate estimates, with which the annual averaged water storage in the major land distributions is assessed. The long-term water budget assessment has proven the hydrological constraints in the MB region under the current climate. These constraints found spatial variations due to an unequal distribution of precipitation over the basin.

From the Budyko curve analysis, we found that AET in the basin is mainly controlled by evaporative demand. This increase in demand makes the basin more arid, and with dwindling freshwater influx, causes the region to be water limited. The long-term climate statistics showed that its spatially averaged annual precipitation is  $\approx 538 \text{ mm yr}^{-1}$ , while water consumption through AET is  $\approx 415 \text{ mm yr}^{-1}$  and runoff is  $123 \text{ mm yr}^{-1}$ , which indicates that the major contribution of AET in the basin is in response to the climate. It is noteworthy to mention that the temporal trend of AET is getting closer to precipitation in the North African base of the Atlas Mountains, where the water budget is  $\approx 0 \text{ mm yr}^{-1}$ , including the Nile delta region, which shows pressure on external water resources. In contrast, the gap between AET and P is wider for Turkey, the Balkans, and the EU, with pronounced runoff patterns. The strong climate variability found in the recent decades for Turkey, the Balkans, and Southern Europe clearly indicates them as more vulnerable to climate effects and affected by irregular patterns.

As a whole, the basin is in a water deficit state due to the strong effect of evaporative demand and the limited water supply to the basin. Since these budget inferences are only based on TerraClimate estimates, which has gained confidence in recent studies, storage biases have not been verified with other global climate products and model-based estimations. The purpose of this study was to show the nature of water balance by already peer-reviewed and published data (TerraClimate) from a first-order perspective. With this, the study opens the opportunity to add more inputs from different model sources for hydrological sub-components, to contribute to the storage calculation over the basin.

Our results suppress the need for continuing serious actions on basin water storage at a large scale, and alarms about escalating climate fluctuations in the MB, especially in Southern Europe, Turkey, and the Balkans. Middle Eastern and North African ecosystems are fragile to water stress where remote sensing-based dynamic water budgeting is preferred for its irrigated, rain-fed, and pastoral land use systems.

**Author Contributions:** Conceptualization, Z.U. and A.G.; methodology, Z.U. and A.G.; data curation, Z.U.; writing—Z.U.; writing—review and editing, Z.U. and B.L.; supervision, M.M. and A.G. All authors have read and agreed to the published version of the manuscript.

**Funding:** This work is funded by (1) the CGIAR Initiative on Climate Resilience, ClimBeR and (2) Regional Water Harvesting Potential Mapping Project under SIDA and FAO.

**Data Availability Statement:** Source code is available on GitHub (<https://github.com/zaib19/Water-Balance-in-the-Mediterranean-Basin-between-1990-and-2020>).

**Acknowledgments:** We acknowledge the doctoral scholarship to Z.U. from the Department of Innovation in Biology, Agri-food and Forest systems (DIBAF), University of Tuscia, Viterbo, Italy. We

are also grateful to the International Center for Agricultural Research in the Dry Areas (ICARDA) for hosting the traineeship to Z.U. Thanks to the National Center for Atmospheric Research at the University of California for sharing the TerraClimate product publicly.

**Conflicts of Interest:** The authors declare no conflict of interest.

## Appendix A

**Table A1.** Class-wise 30-year averaged budget.

Major Class	Minor Class	Area %	P	ET	Q	ΔS
Bare and Open Grazing systems	bare	1.00	910.75	573.36	335.57	0.27
	ext. open rangeland	0.70	444.12	347.12	98.72	0.17
	ext. arid grazing	10.20	243.65	210.90	32.38	0.34
	int. open rangeland	1.80	495.93	383.30	113.22	0.08
	int. arid grazing	8.90	340.33	281.93	58.17	0.05
	Average	Σ 22.6%	486.96	359.32	127.61	0.18
Cropland Systems	ext. annual	10.40	460.19	359.67	100.53	−0.18
	ext. permanent	1.30	608.68	477.60	131.23	−0.22
	ext. annual permanent	2.70	548.40	442.63	105.59	0.11
	rainfed int. annual	5.80	569.68	443.52	126.11	0.07
	rainfed int. permanent	2.20	521.70	435.03	86.37	0.17
	rainfed int. ann. -perm.	1.30	543.74	436.50	107.06	0.26
	irrigated annual	8.70	569.70	430.66	139.38	−0.25
	irrigated permanent	2.20	531.43	440.53	91.00	−0.09
	irri ann. -perm	3.30	511.55	400.23	110.95	0.10
Average	Σ 37.9%	540.56	429.60	110.91	0.00	
Forest systems	medium intensity forest	6.20	837.39	593.49	244.69	−1.03
	semi (natural)	2.60	760.82	549.04	212.35	−0.22
	high intensity	1.00	769.99	561.11	210.02	−0.81
	planted forests	0.30	166.35	150.59	16.45	0.38
	Average	Σ 10.1%	633.63	463.56	170.88	−0.42
Agro-silvo pastoral mosaics	cropland/rangeland	6.50	509.44	405.95	103.49	−0.16
	open woodland	3.20	702.44	514.28	188.24	−0.28
	open wooded rang.	3.50	688.44	505.79	182.84	−0.50
	cropland/wooded rang.	6.80	656.81	501.44	155.72	−0.40
	perm. crops/wooded ran.	1.70	479.15	386.31	92.62	0.00
	closed wooded ran.	1.60	764.19	566.18	198.85	−1.11
	Average	Σ 23.3%	633.41	479.99	153.62	−0.41

## References

- Barredo, J.I.; Mauri, A.; Caudullo, G.; Dosio, A. Assessing shifts of Mediterranean and arid climates under RCP4. 5 and RCP8. 5 climate projections in Europe. In *Meteorology and Climatology of the Mediterranean and Black Seas*; Birkhäuser: Cham, Switzerland, 2019; pp. 235–251.
- Zdruli, P. Land resources of the Mediterranean: Status, pressures, trends and impacts on future regional development. *Land Degrad. Dev.* **2014**, *25*, 373–384. [[CrossRef](#)]
- Vogel, J.; Paton, E.; Aich, V.; Bronstert, A. Increasing compound warm spells and droughts in the Mediterranean Basin. *Weather Clim. Extrem.* **2021**, *32*, 100312. [[CrossRef](#)]
- Hoerling, M.; Eischeid, J.; Perlwitz, J.; Quan, X.; Zhang, T.; Pegion, P. On the increased frequency of Mediterranean drought. *J. Clim.* **2012**, *25*, 2146–2161. [[CrossRef](#)]
- Tramblay, Y.; Llasat, M.C.; Randin, C.; Coppola, E. Climate change impacts on water resources in the Mediterranean. *Reg. Environ. Chang.* **2020**, *20*, 83. [[CrossRef](#)]
- Cardell, M.F.; Amengual, A.; Romero, R. Future effects of climate change on the suitability of wine grape production across Europe. *Reg. Environ. Chang.* **2019**, *19*, 2299–2310. [[CrossRef](#)]
- Milano, M.; Ruelland, D.; Fernandez, S.; Dezetter, A.; Fabre, J.; Servat, E. Facing climatic and anthropogenic changes in the Mediterranean basin: What will be the medium-term impact on water stress? *C. R. Geosci.* **2012**, *344*, 432–440. [[CrossRef](#)]
- Milano, M.; Ruelland, D.; Fernandez, S.; Dezetter, A.; Fabre, J.; Servat, E.; Fritsch, J.M.; Ardoin-Bardin, S.; Thivet, G. Current state of Mediterranean water resources and future trends under climatic and anthropogenic changes. *Hydrol. Sci. J.* **2013**, *58*, 498–518. [[CrossRef](#)]
- Avanzi, F.; Rungee, J.; Maurer, T.; Bales, R.; Ma, Q.; Glaser, S.; Conklin, M. Climate elasticity of evapotranspiration shifts the water balance of Mediterranean climates during multi-year droughts. *Hydrol. Earth Syst. Sci.* **2020**, *24*, 4317–4337. [[CrossRef](#)]
- Ajjur, S.B.; Al-Ghamdi, S.G. Evapotranspiration and water availability response to climate change in the Middle East and North Africa. *Clim. Chang.* **2021**, *166*, 1–28. [[CrossRef](#)]
- Raymond, F.; Ullmann, A.; Tramblay, Y.; Drobinski, P.; Camberlin, P. Evolution of Mediterranean extreme dry spells during the wet season under climate change. *Reg. Environ. Chang.* **2019**, *19*, 2339–2351. [[CrossRef](#)]

12. Abdelwares, M.; Lelieveld, J.; Hadjinicolaou, P.; Zittis, G.; Wagdy, A.; Haggag, M. Evaluation of a regional climate model for the Eastern Nile Basin: Terrestrial and atmospheric water balance. *Atmosphere* **2019**, *10*, 736. [[CrossRef](#)]
13. Bargaoui, Z.; Foughali, A.; Trambly, Y.; Houcine, A. Evaluation of two bias-corrected regional climate models for water budget simulations in a Mediterranean basin. *IAHS-AISH Publ.* **2013**, *359*, 73–79.
14. Santini, M.; Collalti, A.; Valentini, R. Climate change impacts on vegetation and water cycle in the Euro-Mediterranean region, studied by a likelihood approach. *Reg. Environ. Chang.* **2014**, *14*, 1405–1418. [[CrossRef](#)]
15. Oroud, I.M. Water budget assessment within a typical semiarid watershed in the eastern Mediterranean. *Environ. Process.* **2015**, *2*, 395–409. [[CrossRef](#)]
16. Falalakis, G.; Gemitzi, A. A simple method for water balance estimation based on the empirical method and remotely sensed evapotranspiration estimates. *J. Hydroinformatics* **2020**, *22*, 440–451. [[CrossRef](#)]
17. Wong, J.S.; Zhang, X.; Gharari, S.; Shrestha, R.R.; Wheeler, H.S.; Famiglietti, J.S. Assessing water balance closure using multiple data assimilation—and remote sensing—based datasets for Canada. *J. Hydrometeorol.* **2021**, *22*, 1569–1589. [[CrossRef](#)]
18. Zhang, Y.; Pan, M.; Sheffield, J.; Siemann, A.L.; Fisher, C.K.; Liang, M.; Beck, H.E.; Wanders, N.; MacCracken, R.F.; Houser, P.R.; et al. A Climate Data Record (CDR) for the global terrestrial water budget: 1984–2010. *Hydrol. Earth Syst. Sci.* **2018**, *22*, 241–263. [[CrossRef](#)]
19. Sanchez-Gomez, E.; Somot, S.; Mariotti, A. Future changes in the Mediterranean water budget projected by an ensemble of regional climate models. *Geophys. Res. Lett.* **2009**, *36*, L21401. [[CrossRef](#)]
20. Sheffield, J.; Ferguson, C.R.; Troy, T.J.; Wood, E.F.; McCabe, M.F. Closing the terrestrial water budget from satellite remote sensing. *Geophys. Res. Lett.* **2009**, *36*, 07403. [[CrossRef](#)]
21. Zeng, N.; Yoon, J.H.; Mariotti, A.; Swenson, S. Variability of basin-scale terrestrial water storage from a PER water budget method: The Amazon and the Mississippi. *J. Clim.* **2008**, *21*, 248–265. [[CrossRef](#)]
22. Zhao, Y.; Lu, Z.; Wei, Y. An assessment of global precipitation and evapotranspiration products for regional applications. *Remote Sens.* **2019**, *11*, 1077. [[CrossRef](#)]
23. Susanti, I.; Sipayung, S.B.; Siswanto, B.; Maryadi, E.; Latifah, H.; Nurlatifah, A.; Supriatin, L.S.; Witono, A.; Suhermat, M. Implications of extreme events on the water balance in Java. *AIP Conf. Proc.* **2021**, *2331*, 030008. [[CrossRef](#)]
24. Gunkel, A.; Lange, J. Water scarcity, data scarcity and the Budyko curve—An application in the Lower Jordan River Basin. *J. Hydrol. Reg. Stud.* **2017**, *12*, 136–149. [[CrossRef](#)]
25. Luo, Y.; Yang, Y.; Yang, D.; Zhang, S. Quantifying the impact of vegetation changes on global terrestrial runoff using the Budyko framework. *J. Hydrol.* **2020**, *590*, 125389. [[CrossRef](#)]
26. Fang, K.; Shen, C.; Fisher, J.B.; Niu, J. Improving Budyko curve-based estimates of long-term water partitioning using hydrologic signatures from GRACE. *Water Resour. Res.* **2016**, *52*, 5537–5554. [[CrossRef](#)]
27. Singh, R.; Kumar, R. Vulnerability of water availability in India due to climate change: A bottom-up probabilistic Budyko analysis. *Geophys. Res. Lett.* **2015**, *42*, 9799–9807. [[CrossRef](#)]
28. Abera, W.; Formetta, G.; Borga, M.; Rigon, R. Estimating the water budget components and their variability in a pre-alpine basin with JGrass-NewAGE. *Adv. Water Resour.* **2017**, *104*, 37–54. [[CrossRef](#)]
29. Fernandez, R.; Sayama, T. Comparison of future runoff projections using Budyko framework and global hydrologic model: Conceptual simplicity vs process complexity. *Hydrol. Res. Lett.* **2015**, *9*, 75–83. [[CrossRef](#)]
30. Li, Z.; Quiring, S.M. Identifying the dominant drivers of hydrological change in the contiguous United States. *Water Resour. Res.* **2021**, *57*, e2021WR029738. [[CrossRef](#)]
31. Wang, D.; Hejazi, M. Quantifying the relative contribution of the climate and direct human impacts on mean annual streamflow in the contiguous United States. *Water Resour. Res.* **2011**, *47*, W00J08. [[CrossRef](#)]
32. Xu, L. The land surface water and energy budgets over the Tibetan Plateau. *Nat. Preced.* **2011**, *1*. [[CrossRef](#)]
33. Harris, I.P.D.J.; Jones, P.D.; Osborn, T.J.; Lister, D.H. Updated high-resolution grids of monthly climatic observations—the CRU TS3.10 Dataset. *Int. J. Climatol.* **2014**, *34*, 623–642. [[CrossRef](#)]
34. Wang-Erlandsson, L.; Bastiaanssen, W.G.; Gao, H.; Jägermeyr, J.; Senay, G.B.; Van Dijk, A.I.; Guerschman, J.P.; Keys, P.W.; Gordon, L.J.; Savenije, H.H. Global root zone storage capacity from satellite-based evaporation. *Hydrol. Earth Syst. Sci.* **2016**, *20*, 1459–1481. [[CrossRef](#)]
35. Abatzoglou, J.T.; Dobrowski, S.Z.; Parks, S.A.; Hegewisch, K.C. TerraClimate, a high-resolution global dataset of monthly climate and climatic water balance from 1958–2015. *Sci. Data* **2018**, *5*, 1–12. [[CrossRef](#)]
36. Malek, Ž.; Verburg, P. Mediterranean land systems: Representing diversity and intensity of complex land systems in a dynamic region. *Landsc. Urban Plan.* **2017**, *165*, 102–116. [[CrossRef](#)]
37. Budyko, M.I. *Climate and Life*; Academic Press: Orlando, FL, USA, 1974.
38. Yu, Y.; Zhou, Y.; Xiao, W.; Ruan, B.; Lu, F.; Hou, B.; Wang, Y.; Cui, H. Impacts of climate and vegetation on actual evapotranspiration in typical arid mountainous regions using a Budyko-based framework. *Hydrol. Res.* **2021**, *52*, 212–228. [[CrossRef](#)]
39. Adam, J.C.; Clark, E.A.; Lettenmaier, D.P.; Wood, E.F. Correction of global precipitation products for orographic effects. *J. Clim.* **2006**, *19*, 15–38. [[CrossRef](#)]
40. Liakos, C.; Labropoulou, E.; Woodyatt, A. Greece Faces ‘Disaster of Unprecedented Proportions’ as Wildfires Ravage the Country. CNN. Available online: <https://edition.cnn.com/2021/08/09/europe/greece-wildfire-warning-climate-intl/index.html> (accessed on 10 August 2021).

41. Smith, P. Greek Wildfires Are the ‘Harsh Reality of Climate Change,’ Experts Warn. NBCNews. Available online: <https://www.nbcnews.com/news/world/greek-wildfires-are-harsh-reality-climate-change-experts-warn-n1276311> (accessed on 9 August 2021).
42. Pascual, D.; Pla, E.; Lopez-Bustins, J.A.; Retana, J.; Terradas, J. Impacts of climate change on water resources in the Mediterranean Basin: A case study in Catalonia, Spain. *Hydrol. Sci. J.* **2015**, *60*, 2132–2147. [[CrossRef](#)]
43. Rouholahnejad Freund, E.; Kirchner, J.W. A Budyko framework for estimating how spatial heterogeneity and lateral moisture redistribution affect average evapotranspiration rates as seen from the atmosphere. *Hydrol. Earth Syst. Sci.* **2017**, *21*, 217–233. [[CrossRef](#)]
44. Davraz, A.; Sener, E.; Sener, Ş.; Varol, S. Water Balance of the Eğirdir Lake and the Influence of Budget Components, Isparta, Turkey. *Süleyman Demirel Üniversitesi Fen Bilim. Enstitüsü Derg.* **2014**, *18*, 27–36.
45. Ajjur, S.B.; Baalousha, H.M. A review on implementing managed aquifer recharge in the Middle East and North Africa region: Methods, progress and challenges. *Water Int.* **2021**, *46*, 578–604. [[CrossRef](#)]
46. Dezsi, Ş.; Mîndrescu, M.; Petrea, D.; Rai, P.K.; Hamann, A.; Nistor, M.M. High-resolution projections of evapotranspiration and water availability for Europe under climate change. *Int. J. Climatol.* **2018**, *38*, 3832–3841. [[CrossRef](#)]
47. Nangombe, S.; Zhou, T.; Zhang, W.; Wu, B.; Hu, S.; Zou, L.; Li, D. Record-breaking climate extremes in Africa under stabilized 1.5 C and 2 C global warming scenarios. *Nat. Clim. Chang.* **2018**, *8*, 375–380. [[CrossRef](#)]
48. Mariotti, A.; Struglia, M.V.; Zeng, N.; Lau, K.M. The hydrological cycle in the Mediterranean region and implications for the water budget of the Mediterranean Sea. *J. Clim.* **2002**, *15*, 1674–1690. [[CrossRef](#)]
49. Lionello, P.; Malanotte-Rizzoli, P.; Boscolo, R.; Alpert, P.; Artale, V.; Li, L.; Luterbacher, J.; May, W.; Trigo, R.; Tsimplis, M.; et al. The Mediterranean climate: An overview of the main characteristics and issues. *Dev. Earth Environ. Sci.* **2006**, *4*, 1–26.
50. Lelieveld, J.; Hadjinicolaou, P.; Kostopoulou, E.; Chenoweth, J.; El Maayar, M.; Giannakopoulos, C.; Hannides, C.; Lange, M.A.; Tanarhte, M.; Tyrlis, E.; et al. Climate change and impacts in the Eastern Mediterranean and the Middle East. *Clim. Chang.* **2012**, *114*, 667–687. [[CrossRef](#)]
51. Moutahir, H.; Casady, G.; Manrique-Alba, A.; Ruiz-Yanetti, S.; Maturano, A.; Zeram dini, A.; Bellot Abad, J. Can we better understand land surface phenology changes using hydrological variables instead of climate variables. In Proceedings of the XIV MEDECOS & XIII AEET Meeting, Seville, Spain, 31 January–4 February 2017; Volume 31.
52. Llorens, P.; Latron, J.; Gallart, F. Dinámica espacio-temporal de la humedad del suelo en un área de montaña mediterránea. Cuencas experimentales de Vallcebre (Alto Llobregat). *Estud. Zona No Saturada Suelo* **2003**, *6*, 71–76.
53. Ungar, E.D.; Rotenberg, E.; Raz-Yaseef, N.; Cohen, S.; Yakir, D.; Schiller, G. Transpiration and annual water balance of Aleppo pine in a semiarid region: Implications for forest management. *For. Ecol. Manag.* **2013**, *298*, 39–51. [[CrossRef](#)]
54. Mollema, P.; Antonellini, M.; Gabbianelli, G.; Laghi, M.; Marconi, V.; Minchio, A. Climate and water budget change of a Mediterranean coastal watershed, Ravenna, Italy. *Environ. Earth Sci.* **2012**, *65*, 257–276. [[CrossRef](#)]
55. Delle Rose, M.; Martano, P. Datasets of Groundwater Level and Surface Water Budget in a Central Mediterranean Site (21 June 2017–1 October 2022). *Data* **2023**, *8*, 38. [[CrossRef](#)]
56. Scarascia-Mugnozza, G.; Callegari, G.; Veltri, A.; Matteucci, G. Water balance and forest productivity in mediterranean mountain environments. *Ital. J. Agron.* **2010**, *5*, 217–222. [[CrossRef](#)]

**Disclaimer/Publisher’s Note:** The statements, opinions and data contained in all publications are solely those of the individual author(s) and contributor(s) and not of MDPI and/or the editor(s). MDPI and/or the editor(s) disclaim responsibility for any injury to people or property resulting from any ideas, methods, instructions or products referred to in the content.